Assimilation of ATOVS and AMDAR data in the ALADIN 3D-Var system

Roger Randriamampianina, Regina Szoták
Gabriella Csima and Bölöni Gergely
Hungarian Meteorological Service

2003.08.28

1 Introduction

The pre-processing and the implementation of ATOVS (Advanced TIROS Operational Vertical Sounder) and AMDAR (Aircraft Meteorological Data Reporting) data into the ALADIN three-dimensional variational (3D-Var) data assimilation system at the Hungarian Meteorological Service (HMS) was described in Randriamampianina (2003) and Randriamampianina and Csima (2003). This report presents the first results of the study on the impact of ATOVS and AMDAR data on the analysis and forecasts of the ALADIN model.

Section 2 gives brief description of the characteristics of the ALADIN/HU model. Section 3 introduces the pre-processing of ATOVS and AMDAR data. Description of the experiments done for the impact study is shown in Section 4. Subsections 4.1.2 and 4.2.1 present the results of the impact study. In Section 5 we draw some conclusions and discuss further tasks.

2 Main characteristics of the ALADIN/HU model and its assimilation system

The hydrostatic version of the ALADIN model was used in this study. The horizontal resolution of the ALADIN/HU is 6.5 km. ALADIN/HU has 37 vertical levels from surface up to 5 hPa. We use the 3D-Var technique as an assimilation system. An important advantage of the variational technique is that the computation of the cost function for observation part is done in the observation space. Thus, for assimilation of radiances, we have to be able to determine them from the model parameters. For this purpose we need a radiative transfer code. In our case (ARPEGE/ALADIN) we use the RTTOV code (Saunders et al., 1998), which uses 43 vertical levels. Above the top of the model, an extrapolation of the profile is performed using a regression algorithm (Rabier et al., 2001). Below the top of the model, profiles are interpolated to RTTOV pressure levels. Assimilation systems require a good estimation of background error covariance - the so-called "B" matrix. B matrix was computed for the new domain using the "standard NMC method" (Parrish and Derber, 1992). 6 hour assimilation cycling was chosen, consequently the 3D-Var is running 4 times a day at 00, 06, 12 and 18 UTC. We perform 48 hour forecast one time a day from 00 UTC.

3 Data pre-processing

3.1 Pre-processing of the ATOVS data

We receive the ATOVS data through a HRPT antenna. The AMSU-A, level 1C, data are pre-processed by the AAPP (ATOVS and AVHRR Pre-processing Package) package. We use the pre-processing chain Oulan-Bator-Obsort-toODB to create the ODB files. The output of the AAPP is read in direct way in the oulan pre-processing package.

3.1.1 Choice of Satellite:

Because of its technical specification, our antenna receives data from only two satellites at the same time. Data from NOAA-15 are available over the domain of ALADIN/HU at about 06 and 18 UTC, while data from NOAA-16 are available around 00 and 12 UTC. The orbit of the NOAA-17 is between the orbits of the other two satellites a bit closer to that of NOAA-16. We know that NOAA-15 has problem not only with the AVHRR instruments but also with some microwave channels (AMSU-A-11 and AMSU-A-14). Nevertheless, NOAA-15 and NOAA-16 were chosen for the impact study to guarantee the maximum amount of observation at each assimilation time.

3.1.2 Extraction of ATOVS data:

Satellite data observed and pre-processed in the interval of ± 3 hours from the assimilation time are treated. The maximum number of the orbits found at one assimilation time varies up to 3.

3.1.3 Bias correction:

The systematic error of the satellite data can be shown comparing the observed radiances with the computed (simulated) ones. The systematic error arises mainly from errors in the radiative transfer model, instrument calibration problems or biases in the model fields.

The bias correction coefficients for data from NOAA15 and NOAA16 were computed according to Harris and Kelly (2001) for the study period. Note, that the bias coefficients were computed for different latitude bands. Figure 2 demonstrates the bias, computed for the same latitude band for NOAA-15 and NOAA-16.

3.1.4 Channel selection:

Analysing the bias of the brightness temperature, specific for each AMSU-A channel, inside all possible latitude bands, we decided to keep the same number of channels as they were used in the ARPEGE model (see Table 1). Our study is interesting from the point of view of use of AMSU-A data over land (see Table 1), because the percentage of land over the ALADIN-HU domain is more than 70.

3.1.5 Observation statistics and assimilation of radiances:

It is necessary to check the efficiency of ATOVS data based on statistics used to handle the observation in case of new data and, in our case, "new model configuration" (more examples can be seen in Randriamampianina and Rabier, 2001). The observation (AMSU-A radiances) minus guess (computed radiances) were compared with the observation minus analysis for this purpose (Figures 3-6). These figures show statistics computed from a few days (2003.02.20-2003.02.25) cycling. The distance between the two curves indicates how the addition of the AMSU-A data could modify the first-guess fields during the assimilation. The larger the distance the bigger the impact of the observation (so, of the AMSU-A) on the analysis. These results are comparable to those computed in Randriamampianina and Rabier (2001). Another test was done before starting the experiments, which consisted of reproducing the above mentioned experiment after reducing the theoretical standard deviation by half. We did not find any considerable changes in the results. So, we decided to keep the original values of the theoretical standard deviation at this stage as it is used in ARPEGE.

Channel number	1	2	3	4	5	6	7	8	9	10	11	12	13	14	15
Over Land					x	x	x	x	x	x	x	x			
Over Sea					x	x	x	x	x	x	x	x			
Over Sea ice							x	x	x	x	x	x			
Cloudy pixel								x	x	x	x	x			

Table 1: The use of AMSU-A channels. Note, that over land channels 5 and 6 are used when the model orography is less than 500 m and 1500 m, respectively.

3.2 Pre-processing of the AMDAR data

The AMDAR data are pre-processed for 3D-Var every 6 hour. The pre-processing interval is ± 3 hour. Thus, for producing the 12 hour analysis, for instance, we consider AMDAR data, received between 9 and 15 hours. Figure 7 shows the airports in the ALADIN/HU domain. Bold dots indicate places (Frankfurt, Cologne, Hamburg, Berlin, Hanover, Bremen, Rome, Paris, Amsterdam, Venice, Istanbul and Budapest), where the amount of measurements during the study period (2003.02.25-2003.03.01) was outstandingly big. Figures 8 present the spatial locations of all the measurements for a 12 h time interval, corresponding to four (12 and 18 hours) analysis times. As can be seen in the figures, most of aircraft measurements are performed over Western Europe. We use the oulan-bator-obsort-toODB pre-processing chain to insert the AMDAR data into ODB.

4 Experiments design

4.1 Impact of ATOVS data

In the experiments, two thinning distances (80 and 120 km resolution) were investigated. The impact of ATOVS data was studied for a two-week period (from 2003.03.20 to 2003.03.06).

Surface (SYNOP) and radiosonde (TEMP) observations were used in the control run. The impact was evaluated comparing the control run with runs with TEMP, SYNOP and ATOVS data. Examining the first results, we found that the impact of ATOVS data on analysis and forecasts depended on the way the control variables (vorticity, divergence, temperature and surface pressure and the specific humidity) had been handled. In particular, the assimilation of the specific humidity in univariate form or with all control variables using the multivariate formulation.

The following experiments were carried out:

T8000 - TEMP, SYNOP and AMSU-A data were assimilated. The AMSU-A data were thinned at 80 km resolution. The multivariate formulation was used for all control variables.

T1200 - TEMP, SYNOP and AMSU-A data were assimilated. The AMSU-A data were thinned at 120 km resolution. The multivariate formulation was used for all control variables.

Aladt - TEMP and SYNOP were assimilated - control run. It is our 3D-Var cycling running in parallel suite. The multivariate formulation was used for all control variables.

Touhu - TEMP, SYNOP and AMSU-A data were assimilated. The AMSU-A data were thinned at 80 km resolution. The specific humidity was assimilated in form of univariate control variable, when the other control variables were assimilated using multivariate formulation.

12uhu - TEMP, SYNOP and AMSU-A data were assimilated. The AMSU-A data were thinned at 120 km resolution. The specific humidity was assimilated as an univariate control variable, when the other control variables were assimilated using multivariate formulation.

Aluhu - TEMP and SYNOP were assimilated - the control run. The specific humidity was assimilated as an univariate control variable, when the other control variables were assimilated using multivariate formulation.

Dynam - Dynamical adaptation run - the operational run in Hungary.

4.1.1 Objective verification:

This report presents the results of the objective verification. The bias and the root mean square error (RMSE) were computed from the differences between the analysis/forecasts and the observations (SYNOP and TEMP).

4.1.2 Most important results

4.1.3 Using multivariate formulation:

- We found that AMSU-A data have positive impact on the analysis and forecasts of geopotential height when assimilating them in both 80 and 120 km resolutions. Especially, on lower levels (i.e. below 700 hPa), the impact was positive for all forecast ranges. Positive impact on the short-range (until 12 hour) forecast was observed for all model levels (see Fig. 9).
- A neutral impact on the analysis and forecasts of wind speed was observed.
- A neutral impact of AMSU-A data on the temperature profile was found.
- Regarding the relative humidity fields, negative impact was observed.

The "stability" of the negative impact of AMSU-A data on relative humidity fields showed that the source might have come from the way the humidity measurements had been assimilated. We decided to separate the specific humidity from the multivariate formulation and assimilate it alone (univariate form).

4.1.4 Assimilating the humidity in univariate form:

- The impact of AMSU-A data on forecast of geopotential height was somewhat less, but positive compared to the run with multivariate formulation.
- Positive impact on the temperature above 700 hPa was observed from the 24 hour forecast range (see Fig. 10)
- Concerning the impact on relative humidity, improvement could be observed (Fig. 11). It is important to mention that we found big improvement at all model levels when assimilating the humidity data in univariate form, especially for levels around the tropopause (see Fig. 12). It can be also observed on the run without ATOVS data (see Fig. 13).
- A neutral impact was found for the wind speed.

4.1.5 Influence of resolution:

We performed comparisons to evaluate the influence of resolution of ATOVS data on analysis and forecast. In general, the positive impact of ATOVS data on geopotential and temperature was stronger in case of finer (80 km) resolution of ATOVS data. The 120 km resolution gave "better" impact on relative humidity, wind speed and wind direction when using multivariate formulation. Assimilating the humidity data in univariate form, the finer resolution gave "better" impact on relative humidity (see Fig. 14).

We concluded, that the positive impact was somewhat stronger in general when ATOVS data were assimilated at finer resolution, especially when the specific humidity was assimilated in univariate form.

4.1.6 Comparison of 3D-Var and dynamical adaptation:

We can conclude that the 3D-Var analysis of wind, geopotential and humidity fields was closer to the observation compared to the ARPEGE analysis (see Fig. 15), which is the initial condition for the dynamical adaptation. However the dynamical adaptation gave better results on forecasts of temperature for lower levels (see Fig. 16).

4.1.7 Selected cases

We concluded, that the impact of ATOVS data on the forecast on different parameters was slightly positive or neutral in general. In the following, we chose certain cases within the studied period to compare the runs with and without ATOVS data with a special attention on forecast of precipitation. Exploring the reasons of negative impact on the forecast of humidity it was ascertained, that in some cases no ATOVS data was available at all (e.g. 24 February, see Fig. 17), or the negative impact was characteristic for territories, located rather far from the satellite pass (e.g. 28 February, see later). It indicates, that the negative impact may refer to the absence of ATOVS data, so that the ATOVS data did not have the possibility to correct the "bad quality" first-guess fields.

We examined what differences we receive in the spatial distribution of cumulative precipitation depending on the use (here we mean inclusion or exclusion) of the ATOVS data in the 3D-Var runs. The results of this study are given in Figures 18-23.

Figures 18 and 19 show that from the synoptical point of view, there is no big differences between the maps, created from results of the runs with (below) and without (above) ATOVS data. The objective verification, however, showed positive impact (Fig. 17) of ATOVS data on the humidity on this particular day (2 March).

Figures 20 and 21 show differences in cumulative precipitation between the runs with (below) and without (above) ATOVS data at the Easterin cost of Poland and Western part of Byelorussia. According to the real situation, presented in Figure 21, there was some precipitation over the mentioned area. One can see that the run with ATOVS data could slightly better describe this situation (4 March).

In Figures 20 and 23 we examined a situation, when ATOVS data were available over a very small part of the ALADIN/HU domain. Analysing the 24 hour cumulative precipitation, one can say that the run with ATOVS data gave poorer results than the run without ATOVS data for cases, when the rainy territories (W-SW) were located far away from the satellite pass (E). Moreover, in Figure 17 (see the 24 h. forecast on Feb. 28 as an example) one can see, that the impact of ATOVS data was slightly negative.

Detailed analyses of the above mentioned cases provide important additional information for the impact study compared to statistical evaluation. Thus, the indexes of the objective verification sometimes might be not enough for thorough assessment of the impact of satellite data on analysis and forecast.

4.2 Impact of AMDAR data

In the experiments, two thinning techniques (170 and 50 km resolution) were investigated. 50 km resolution was chosen based on the results of the investigation on the thinning of the aircraft data desribed in (Kertész and Fischer, 2001) (see Fig. 24). It is shown on this graph that, at best, we can use more than 50 percent of the incoming AMDAR data, by reducing the thinning distance, at least, to 50 km. The impact of AMDAR data was studied for a two-week period (from 2003.04.18 to 2003.05.07). Surface (SYNOP) and radiosonde (TEMP) observations were used in the control run. The impact was evaluated comparing the control run with runs with TEMP, SYNOP and AMDAR data. Due to the problem related to the assimilation of the humidity (described reviously), experiments were done assimilating the specific humidity in univariate form and together with all control variables (multivariate formulation).

The following experiments were carried out:

am170 - TEMP, SYNOP and AMDAR data were assimilated. The AMDAR data were thinned at 170 km resolution. The multivariate formulation was used for all control variables.

amd50 - TEMP, SYNOP and AMDAR data were assimilated. The AMDAR data were thinned at 50 km resolution. The multivariate formulation was used for all control variables.

Aladt - TEMP and SYNOP were assimilated - control run. It is our 3D-Var cycling running in parallel suite. The multivariate formulation was used for all control variables.

uamd - TEMP, SYNOP and AMDAR data were assimilated. The AMDAR data were thinned at 170 km resolution. The specific humidity was assimilated in form of univariate control variable, when the other control variables were assimilated using multivariate formulation.

aluhu - TEMP, SYNOP and AMDAR data were assimilated. The AMDAR data were thinned at 170 km resolution. The specific humidity was assimilated as an univariate control variable, when the other control variables were assimilated using multivariate formulation.

4.2.1 Most important results

4.2.2 Using the multivariate formulation:

Using the multivariate formulation, two impact studies at 170 km and 50 km resolutions were performed with the AMDAR data. Neutral impacts on the analysis and forecast were found in both cases. However, the impact of AMDAR data was slightly "better" when using AMDAR data at finer (50 km) resolution (Fig. 25).

4.2.3 Assimilation the specific humidity in univariate form:

On preliminary experiment was performed to estimate the impact of AMDAR data on the analysis and forecast when assimilating the specific humidity in univariate form. We found slightly better impact in this case compared to the multivariate one (Fig. 26).

We compared the amount of AMDAR profiles at each assimilation time compared to TEMP ones. The smallest amount of AMDAR data was found at 00UTC (Table 2) for the study period. Thus, the reason of the neutral or slightly positive impact of the AMDAR data could be the small amount of AMDAR profiles at the chosen prediction time.

Analysis time	00 UTC	06 UTC	12 UTC	18 UTC
Relative amount	0.15	4.50	0.80	5.00

Table 2: Relative amount of AMDAR profiles compared to TEMP ones for the period from 2003.04.18 to 2003.05.07.

5 Summary, further suggestions and experiments

5.1 Concerning the ATOVS data

- The assimilation of the ATOVS data into the limited area model ALADIN/HU gave neutral impact in general (the positive and negative impacts were slight).
- Because of the problems related to the humidity, it is recommended to assimilate the humidity data in univariate form. We changed the assimilation of the humidity from multivariate to univariate in the version of 3D-Var, running actually in parallel suite in Budapest.
- The impact of the ATOVS data on the forecast of temperature was slightly negative in the lower levels. To avoid so, it is recommended to investigate the use of channels, sensitive to the lower atmospheric layers (channels 5, 6 and 7) before performing any further experiments.
- Since the impact of ATOVS data with finer (80 km) resolution was somewhat "better", than that of 120 km resolution data, it is recommended to perform the further assimilation of ATOVS data in finer resolution.
- It would be necessary to perform similar experiment for other periods as well.
- We suggest to perform further experiments to study the changes in the impact of ATOVS data on the forecast in extreme weather conditions.

5.2 Concerning the AMDAR data

- We concluded, that the AMDAR data could provide additional information mainly at 06, 12 and18 UTC analysis times.

- The preliminary impact study showed neutral or slightly positive impact of AMDAR data on the analysis and forecast.
- Slightly positive impact of the AMDAR data on the analysis and forecast was found when assimilating the specific humidity in univariate form.
- The uncertainty of the results suggests to investigate the efficiency of the assimilation of the AMDAR data (evaluation of observation minus guess and observation minus analysis) before doing any further impact studies. This would result evaluation of the observation errors.
- It would be very important to study the influence of reduced thinning distances. It is also recommended to investigate the extraction of the AMDAR data within shorter time interval or assimilate them with shorter (for example 3 hour) cycling.

  Summing up we can state, that at the present stage no definite positive impact of ATOVS or AMDAR data on the forecast can be proved in the 3D-var data assimilation system of the ALADIN model, so it is necessary to continue the experiments.

Acknowledgements

The authors wish to thank Florence Rabier, Élisabeth Gérard, Philippe Caille, Jean-Marc Audouin and Hungarian colleagues from the System Management Division, HMS, for their help and fruitful discussion. Partial support for this work has been provided by the Hungarian Scientific Joint Foundation OTKA T031865 and T032466.

References

[1] Harris, B. A. and Kelly, G., 2001: *A satellite radiance-bias correction scheme for data assimilation*, Q.J.R. Meteorol. Soc., 127, 1453-1468

[2] Sandor Kertész and Claude Fischer, 2001: *Observation management for ALADIN*, ALADIN internal report, available at Météo-France and at HMS.

[3] Roger Randriamampianina and Florence Rabier, 2001: *Use of locally received ATOVS radiances in regional NWP.* NWP SAF report, available at HMS and at Météo-France.

[4] Roger Randriamampianina, 2003: *Investigation of the use of local ATOVS data in Budapest*, ALADIN Newsletter N. 23, 2003.

[5] Roger Randriamampianina and Gabriella Csima, 2003: Pre- processing of the AMDAR data at HMS, ALADIN Newsletter N. 24, 2003.

[6] F. Rabier, É. Gérard, Z. Shlaoui, M. Dahoui, R. Randriamampianina, 2001: *Use of ATOVS and SSMI observations at Météo-France.* 11th Conference on Satellite

Meteorology and Oceanography, Madison, WI, 15-18 October 2001 (preprints). Boston, MA, American Meteorological Society, pp367-370.

[7] Parrish, D. F. and J. C. Derber, 1992: *The National Meteorological Centre's spectral statistical interpolation analysis system.* Mon. Wea. Rev., 120, 1747-1763

[8] Sounders, R, M. Matricardi and P. Brunel, 1999: *An improved fast radiative transfer model for assimilation of satellite radiance observations.* Q.J.R. meteorol. Soc., 125, 1407-1425

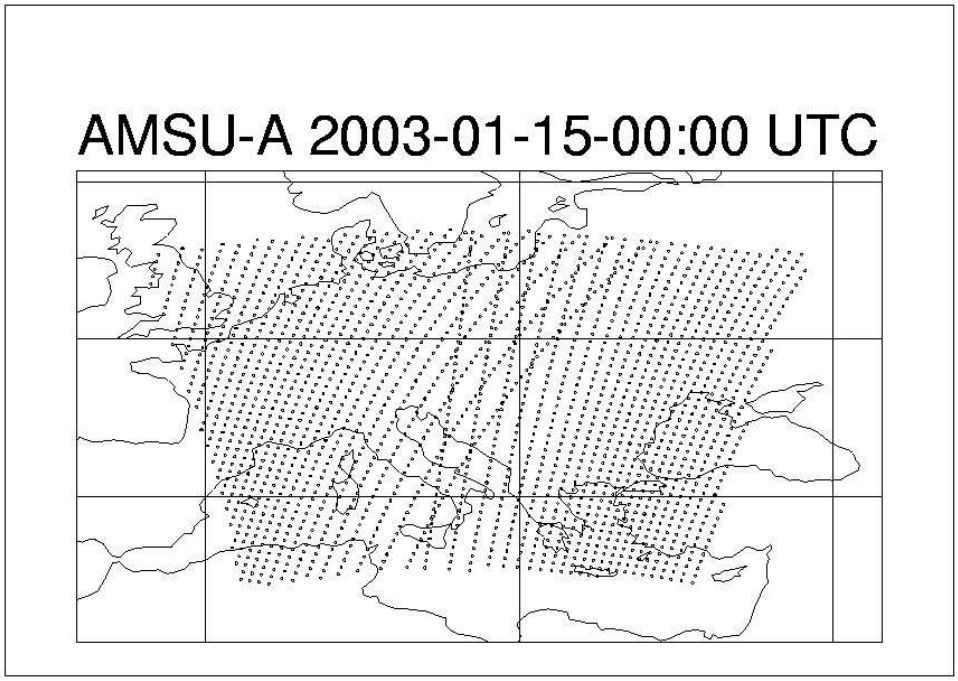

Figure 1: Satellite data over the ALADIN-HU domain (C+I zone).

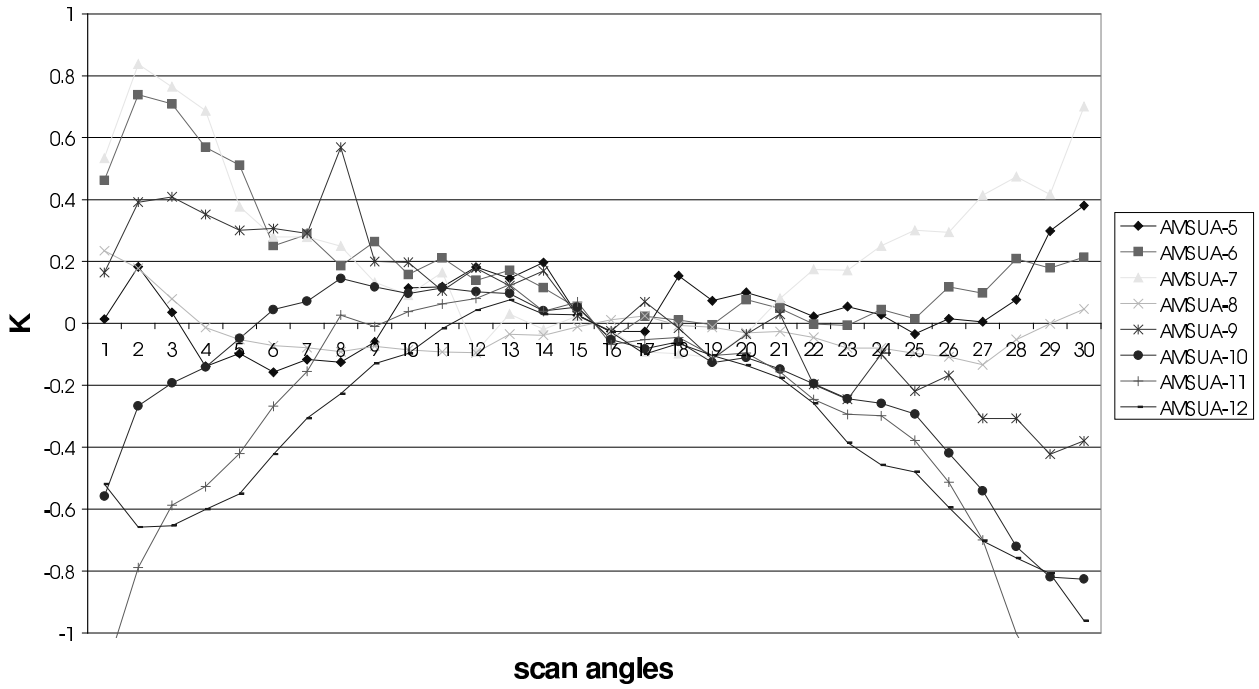

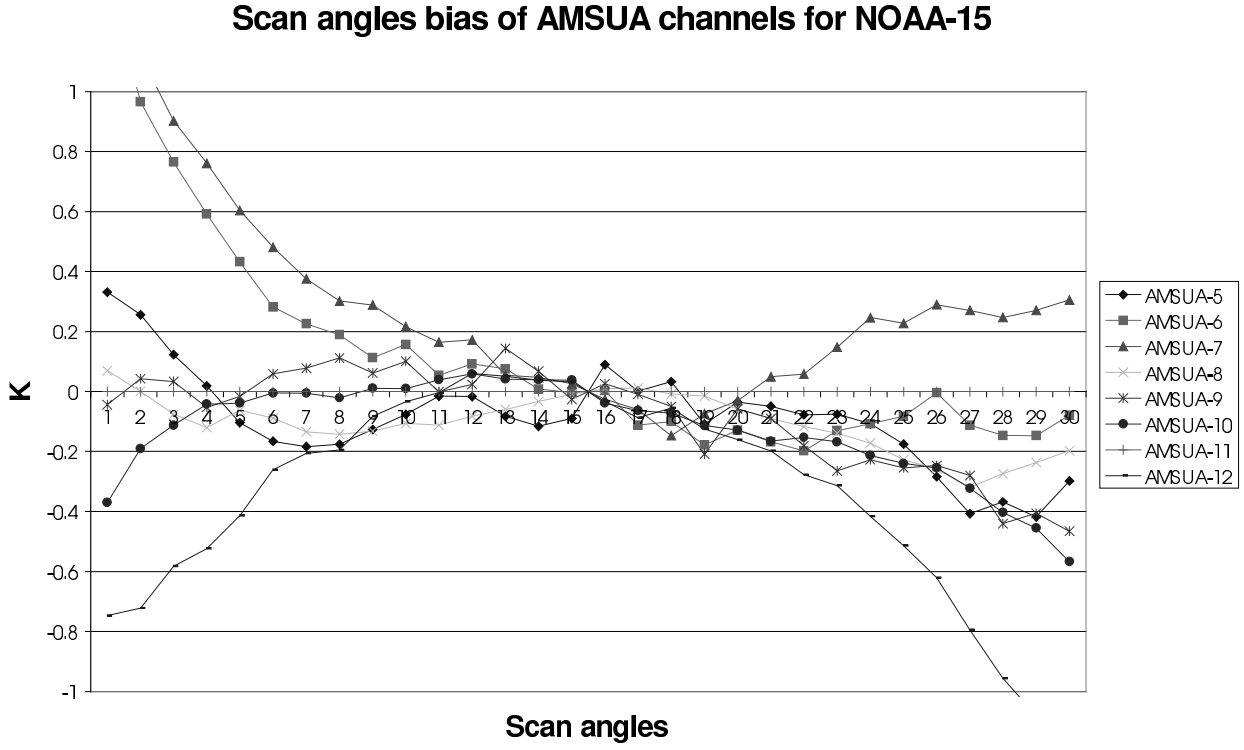

Figure 2: Bias (in Kelvin degree) specific to the scan angles varies with latitude band. In these figures biases were computed for the same latitude band.

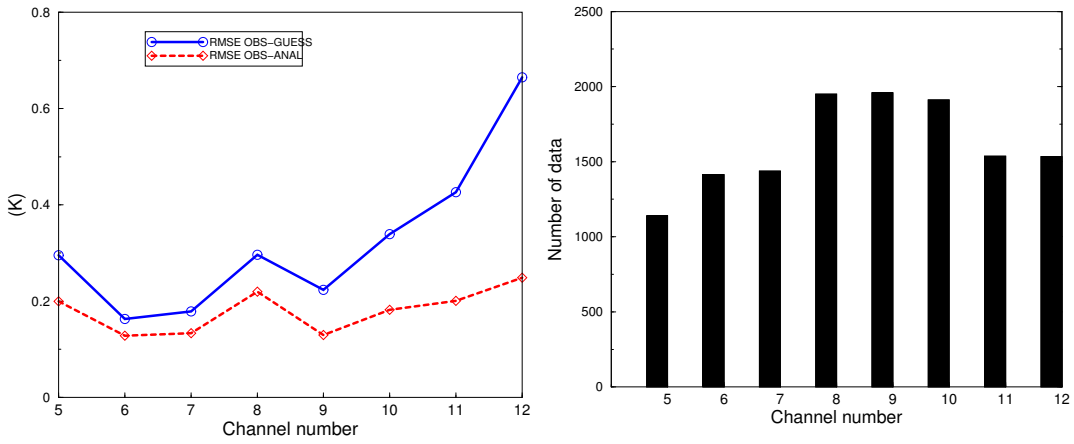

Figure 3: Example of statistics of observation minus guess (solid line) and observation minus analysis (dashed line) for AMSU-A at 00 UTC for a five days cycling (from 2003.02.20 to 2003.0225) (left hand side). On the right one can find the number of data used in the computation of the statistics. The impact of AMSU-A is larger at higher layers of the atmosphere (channels 9-12).

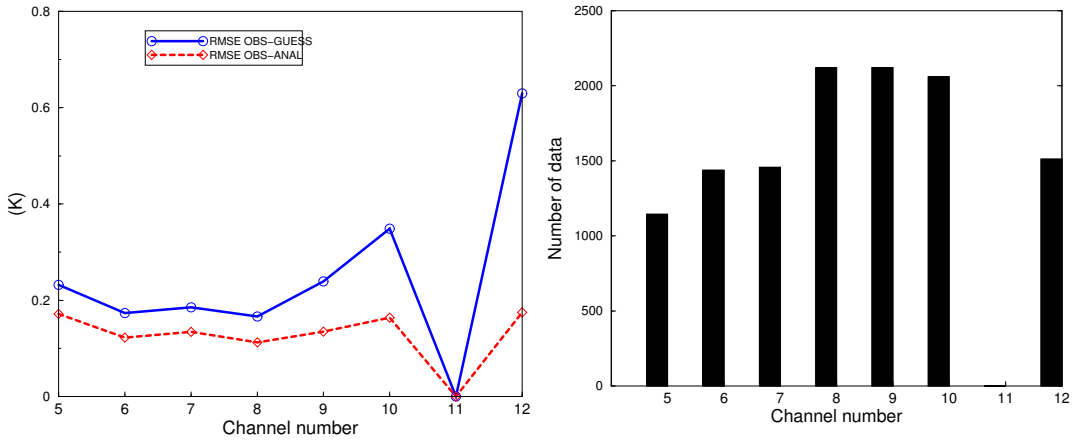

Figure 4: Example of statistics of observation minus guess (solid line) and observation minus analysis (dashed line) for AMSU-A at 06 UTC for a five days cycling (from 2003.02.20 to 2003.0225) (left hand side). On the right one can find the number of data used in the computation of the statistics. Note, that around 06 UTC we receive data from NOAA-15, which has problem with AMSU-A channel 11. The impact of AMSU-A is larger at higher layers of the atmosphere (channels 9-12).

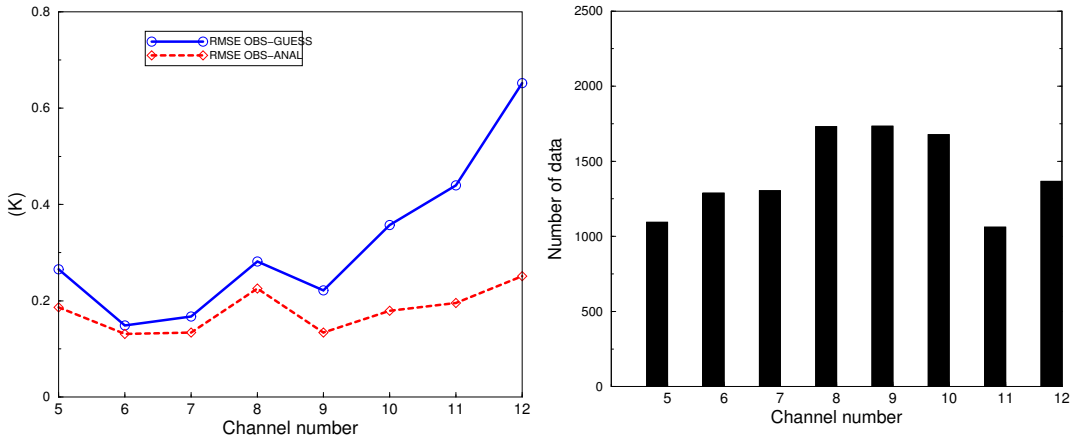

Figure 5: Example of statistics of observation minus guess (solid line) and observation minus analysis (dashed line) for AMSU-A at 12 UTC for a five days cycling (from 2003.02.20 to 2003.0225) (left hand side). On the right one can find the number of data used in the computation of the statistics. The impact of AMSU-A is larger at higher layers of the atmosphere (channels 9-12).

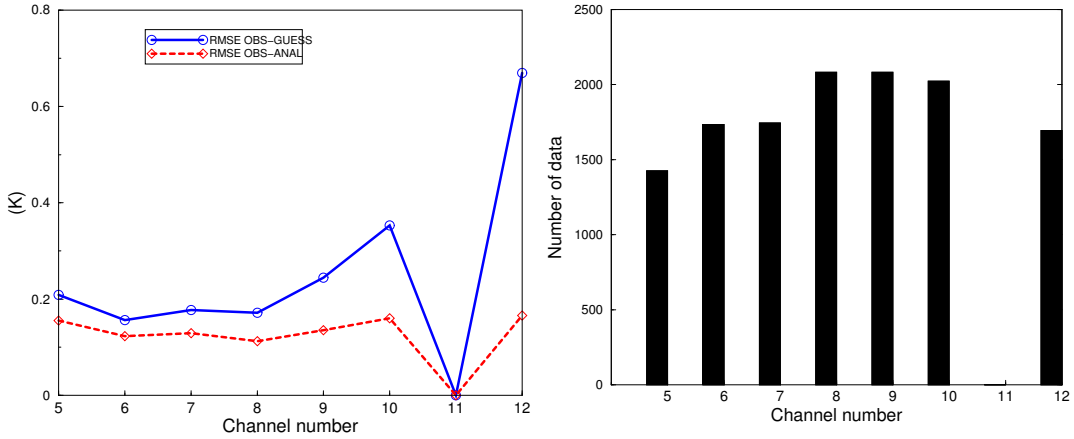

Figure 6: Example of the statistics of the observation minus guess (solid line) and the observation minus analysis (dashed line) for AMSU-A at 18 UTC(left hand side). On the right one can find the number of data used in the computation of the statistics. Note, that around 18 UTC we receive data from NOAA-15, which has problem with AMSU-A channel 11. The impact of AMSU-A is larger at higher layers of the atmosphere (channels 9-12).

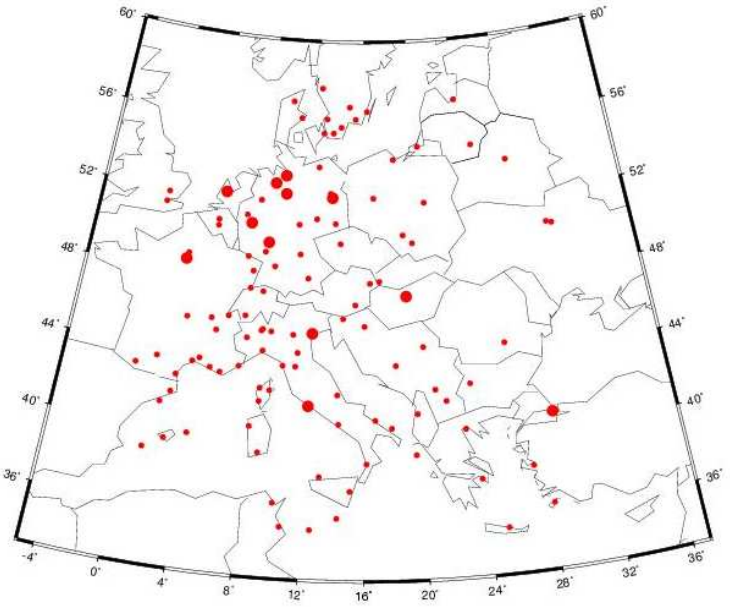

Figure 7: Location of airports in the ALADIN-HU domain. Bold dots indicate places with big amount of AMDAR measurements.

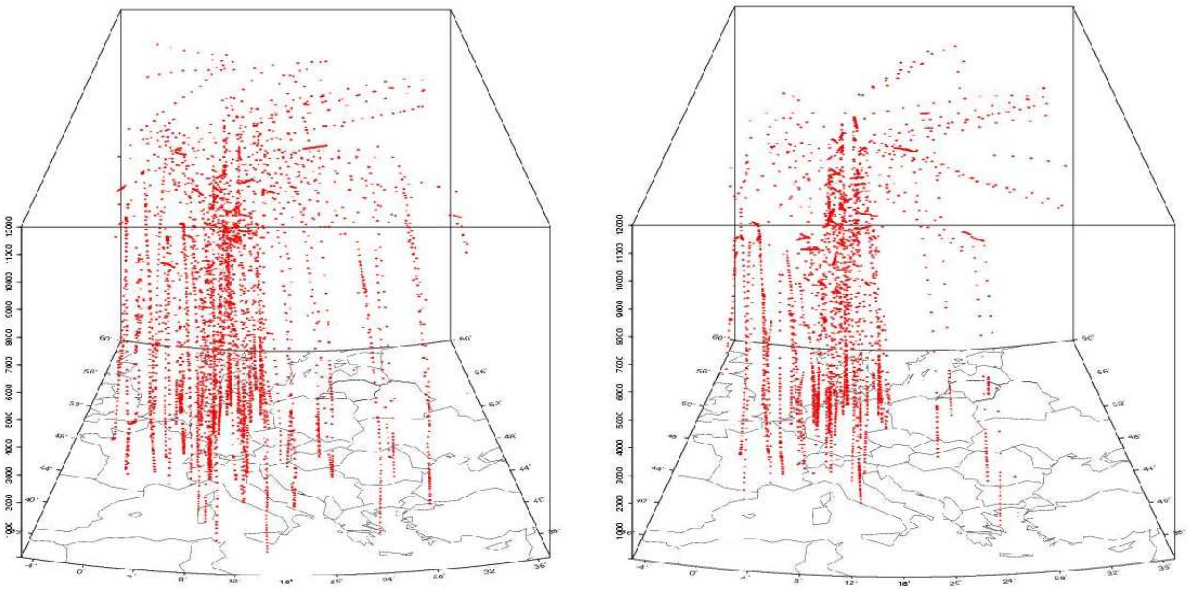

Figure 8: Spacial tree-dimentionnal distribution of AMDAR measurements (during landing and take off) over ALADIN/HU domain within a ± 3 hour interval at 12 UTC (left) and 18 UTC (right)(2003.02.25) assimilation time.

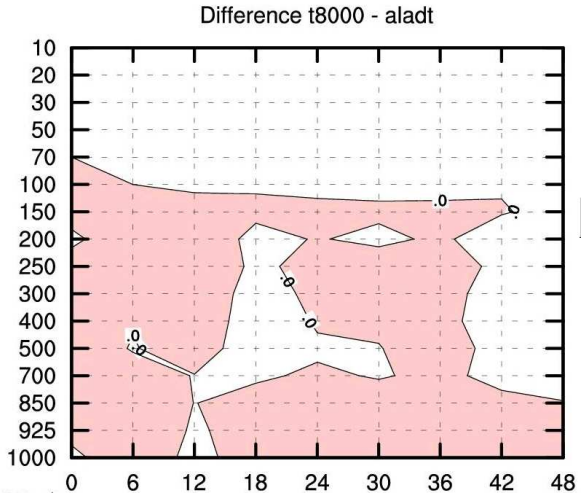

Figure 9: Difference between the root mean square errors for geopotential height: $RMSE_{T8000} - RMSE_{Aladt}$. Negative value (coloured) means that the error of run with ATOVS data is less than that of control run, thus the ATOVS data have positive impact. X and Y axes present the forecast ranges and the model levels respectively.

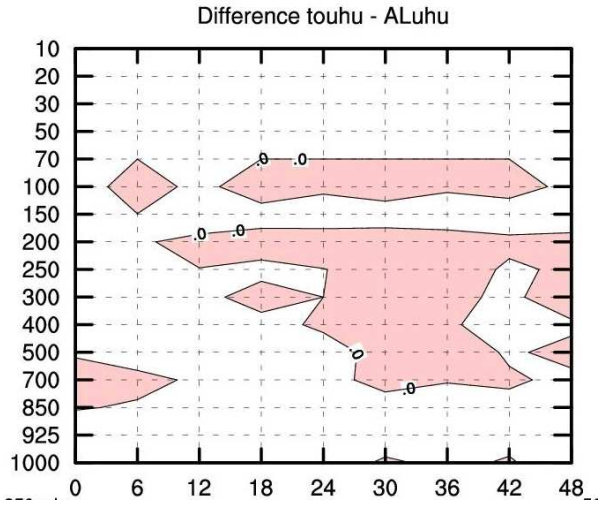

Figure 10: Difference between the root mean square errors of temperature in case of assimilating the humidity data in univariate form: $RMSE_{Touhu} - RMSE_{Aluhu}$. Negative value (coloured) means that the error of run with ATOVS data is less than that of control run, thus the ATOVS data have positive impact. X and Y axes present the forecast ranges and the model levels respectively.

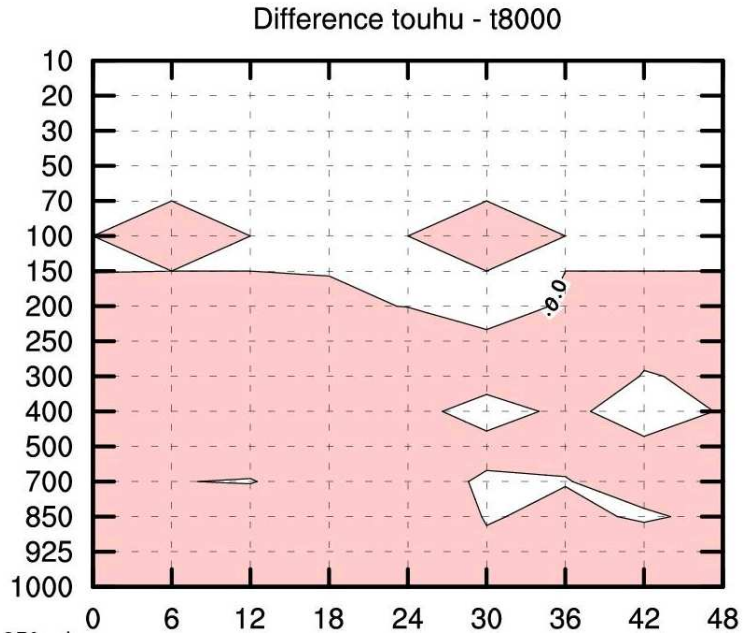

Figure 11: Difference between the root mean square errors of relative humidity: $RMSE_{Touhu} - RMSE_{T8000}$. Negative value (coloured) means that the error is reduced when assimilating the specific humidity in univarite form.

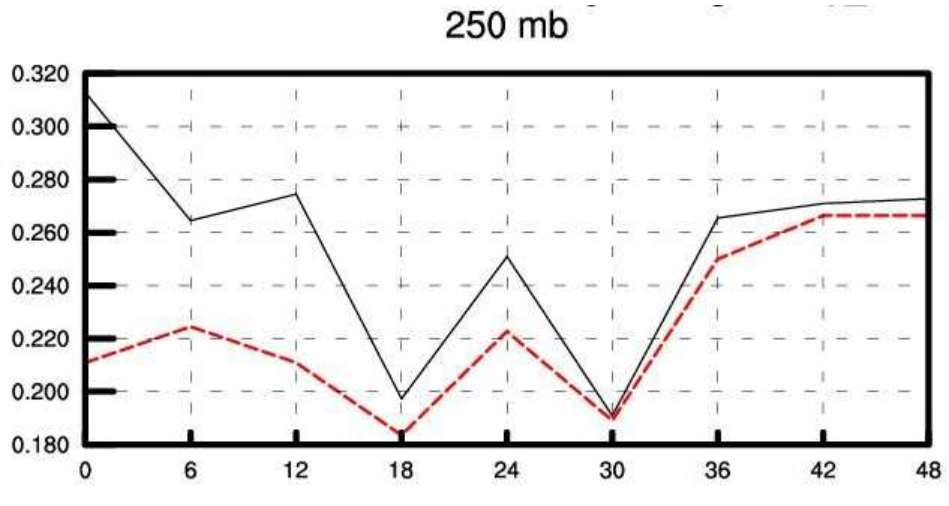

Figure 12: Root mean square forecast errors of relative humidity (in percent) at 250 hPa level against radiosonde observation. Comparison of two 3D-Var runs with ATOVS data assimilated in 80 km resolution. Solid line: when the multivariate formulation was used for all control variables ($T800$). Dashed line: when the specific humidity was assimilated in univariate form ($touhu$). X axis presents the forecast ranges in hour.

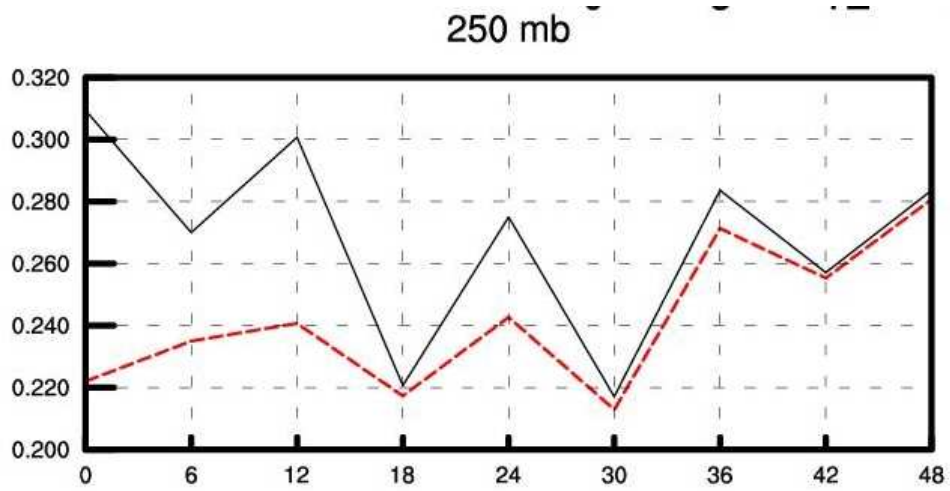

Figure 13: Root mean square forecast errors of relative humidity (in percent) at 250 hPa level against radiosonde observation. Comparison of two 3D-Var runs with TEMP and SYNOP data. Solid line: when the multivariate formulation was used for all control variables (*aladt*). Dashed line: when the specific humidity was assimilated in univariate form (*aluhu*, dashed line). X axis presents the forecast ranges in hour.

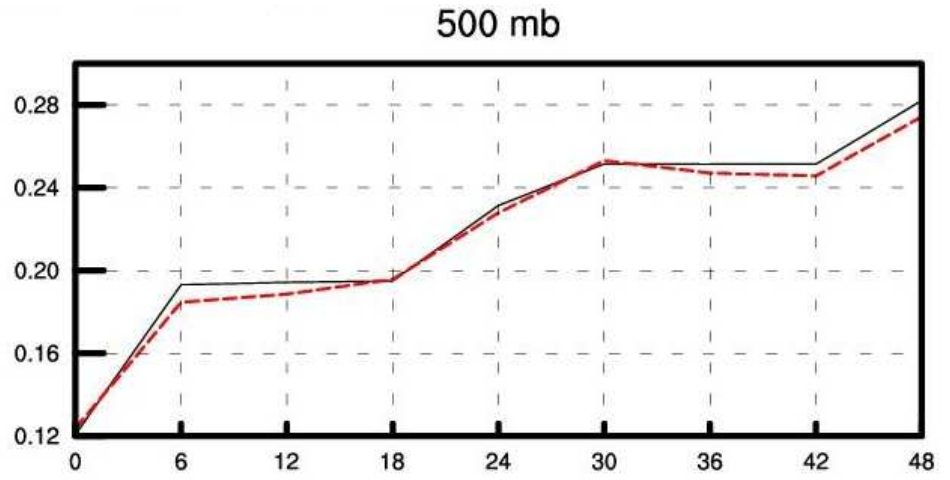

Figure 14: Root mean square forecast errors of relative humidity (in percent) at 500 hPa level against radiosonde observation. Comparison of two 3D-Var runs with ATOVS data when the humidity was assimilated in univariate form. Dashed line: thinning in 80 km (*touhu*). Solid line: thinning in 120 km (120*uhu*). X axis presents the forecast ranges in hour.

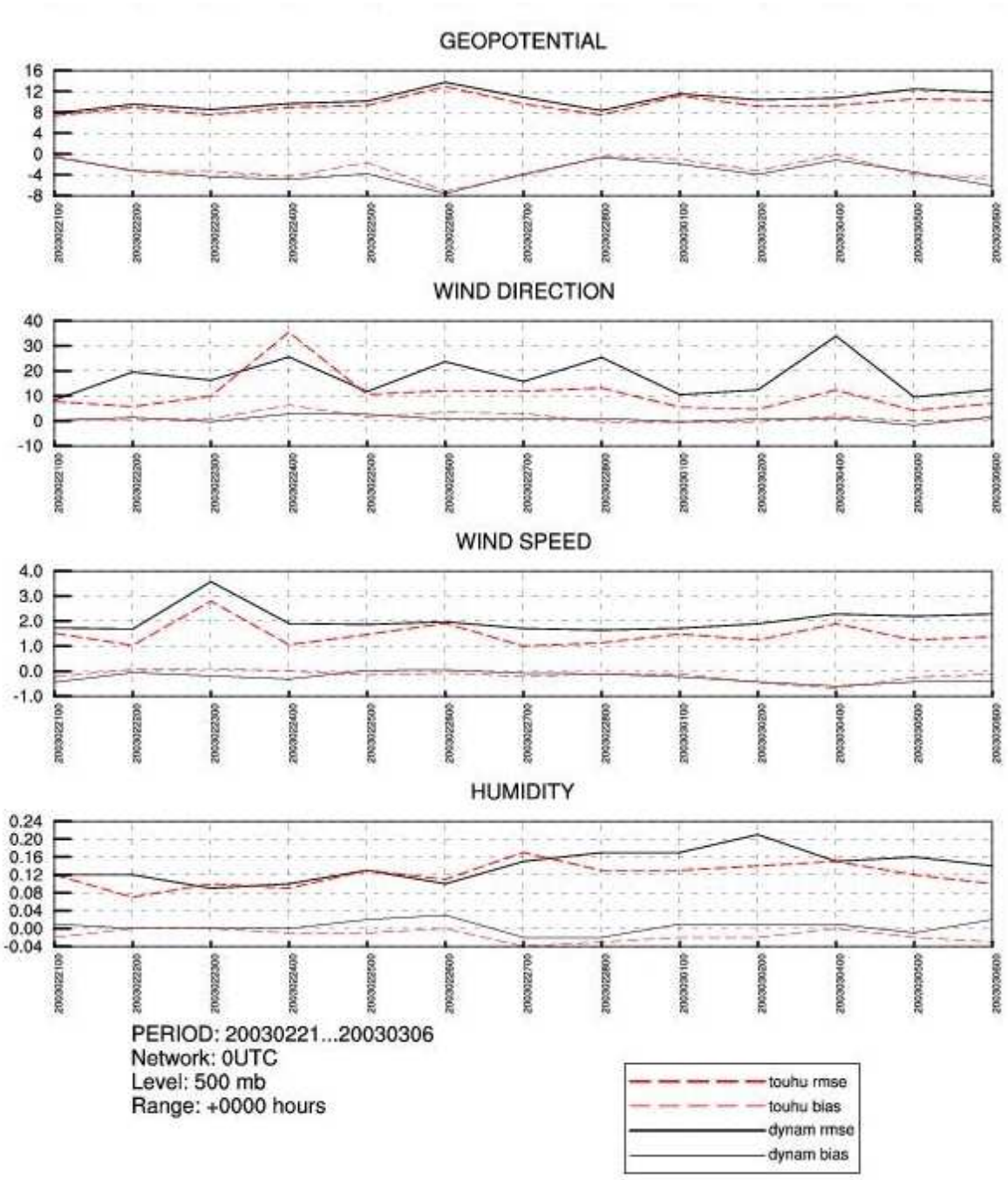

Figure 15: Comparison of day-to-day statistics (RMSE - upper curves and bias - lower curves) of dynamical adaptation run (*dynam*, solid line) and 3D-Var run with ATOVS data assilimilated in 80 km resolution (*touhu*, dashed line). The statistics correspond to 500 hPa model level.

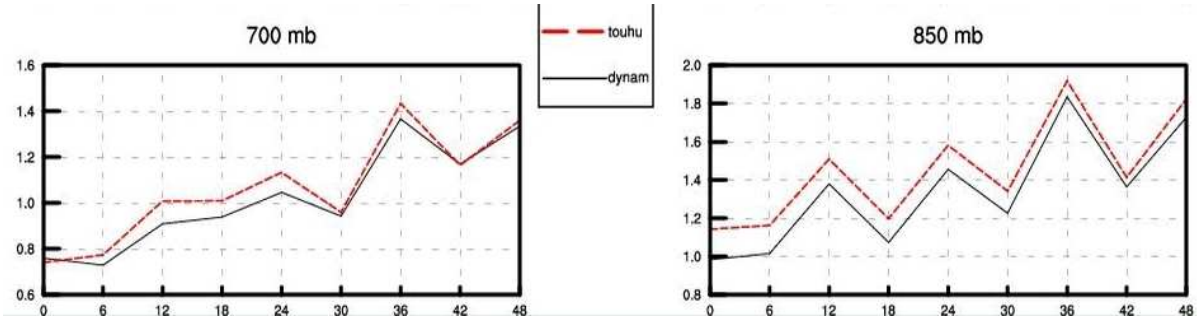

Figure 16: Root mean square forecast errors of temperature (in Kelvin) at 700 and 850 hPa model levels. Comparison of scores of a dynamical adaptation (*dynam*, solid line) and a 3D-Var with ATOVS data assimilated in 80 km resolution (*touhu*, dashed line). X axis presents the forecast ranges in hour.

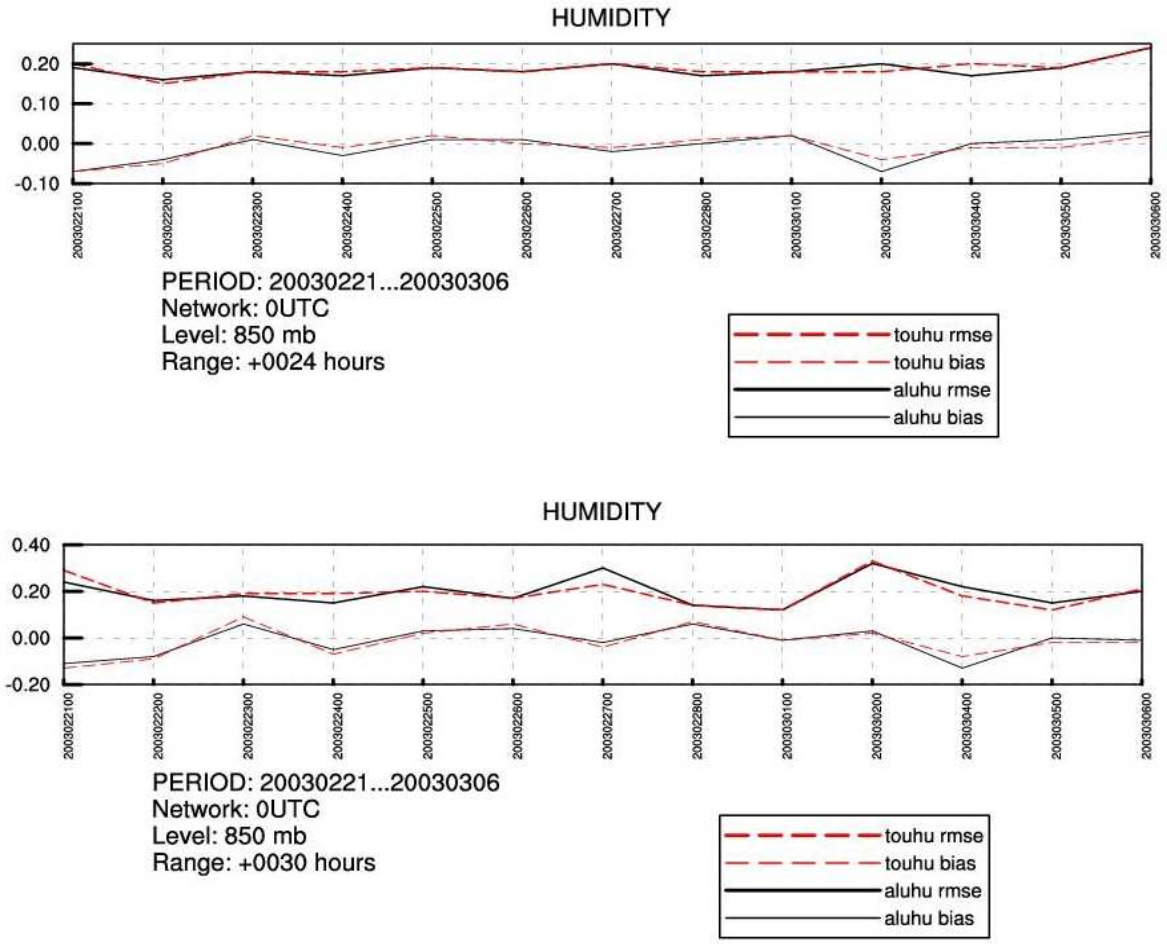

Figure 17: Day-to-day root mean square forecast errors (upper curves) and biases (lower curves) of relative humidity at 850 hPa model level. Comparison of 3D-Var run with ATOVS data assimilated in 80 km (*touhu*, dashed line) with the control one (with TEMP and SYNOP only) (*aluhu*, solid line) for 24 (upper graphic) and 30 (lower graphic) hour forecast ranges.

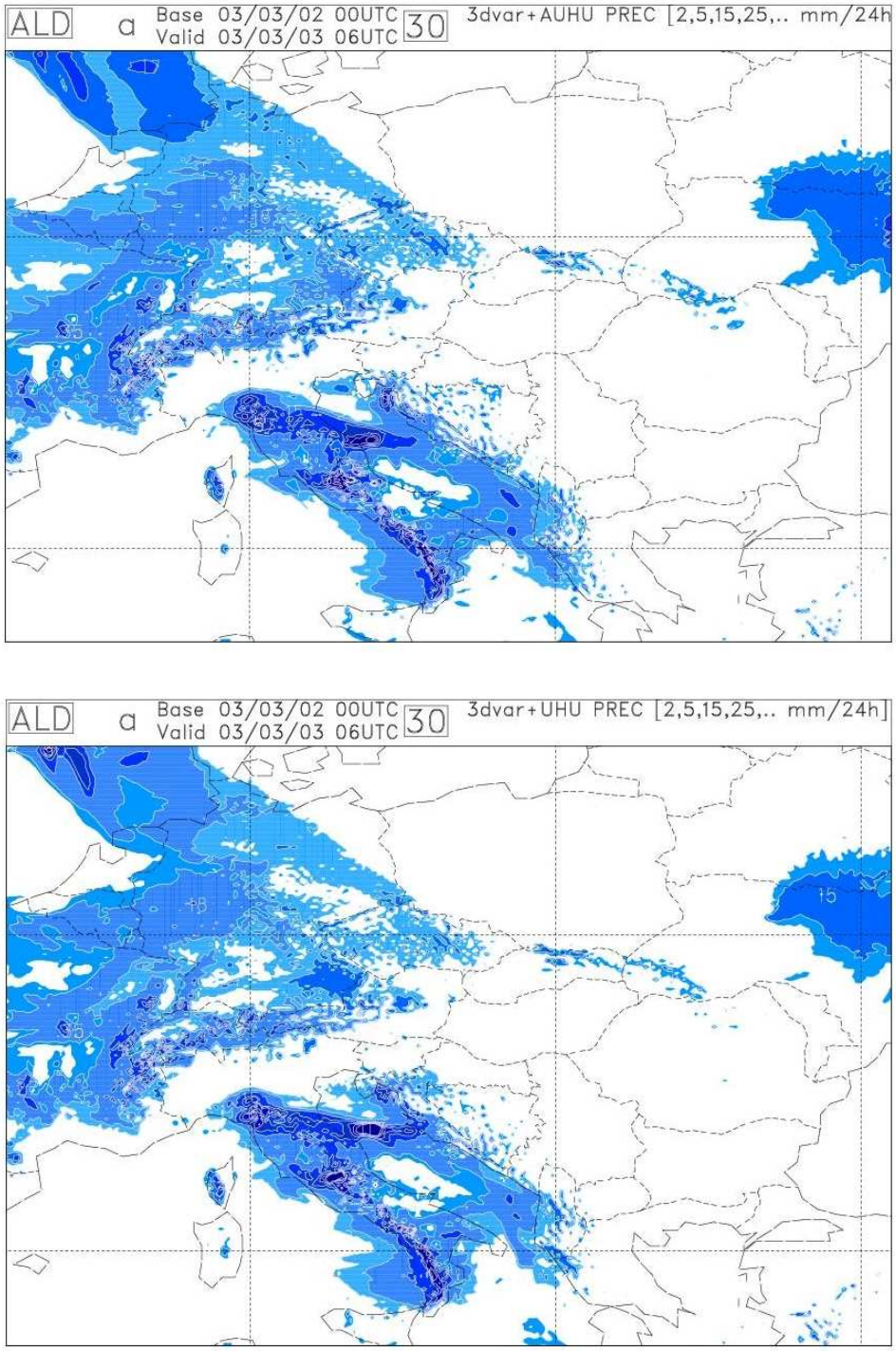

Figure 18: The 24 hour cumulative precipitation (in mm) predicted over the ALADIN/HU domain from 2003.03.02 00 UTC. Upper picture: control run (with TEMP and SYNOP). Lower picture: 3D-Var run with ATOVS assimilated in 80 km resolution. In both runs the humidity was assimilated in univariate form. Note that the 24 hour cumulated precipitation is the difference between the cumulative precipitation predicted at 6 and 30 hour forecast ranges.

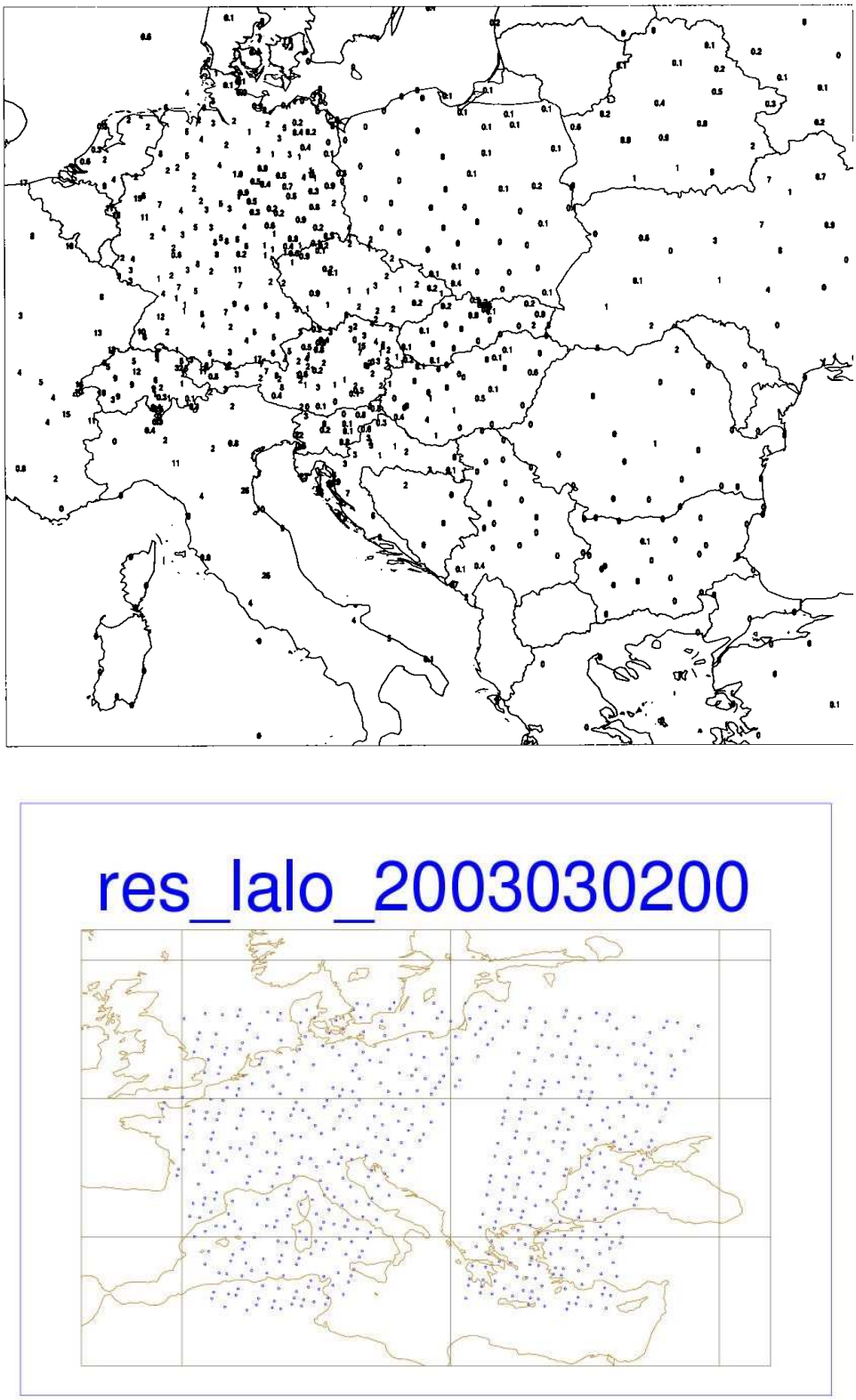

Figure 19: The 24 hour cumulative precipitation (in mm) extracted from SYNOP telegrams for 2003.03.03 06 UTC (upper picture) and the distribution of the ATOVS pixels 2003.03.02 00 UTC (situation after screening - active observation) (lower picture).

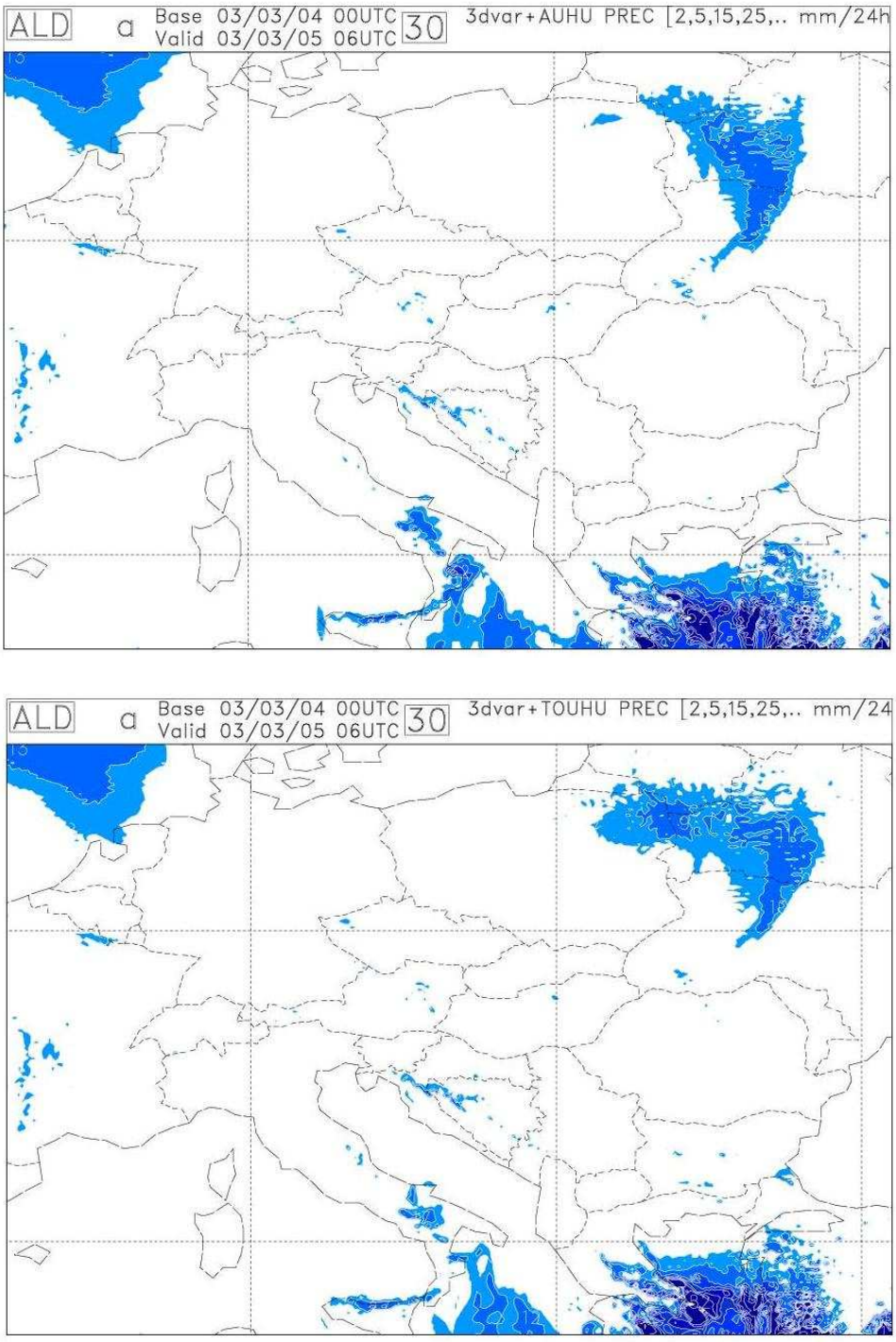

Figure 20: The 24 hour cumulative precipitation (in mm) predicted over the ALADIN/HU domain from 2003.03.04 00 UTC. Upper picture: control run (with TEMP and SYNOP). Lower picture: 3D-Var run with ATOVS assimilated in 80 km resolution. In both runs the humidity was assimilated in univariate form. Note that the 24 hour cumulated precipitation is the difference between the cumulated precipitation predicted at 6 and 30 hour forecast ranges.

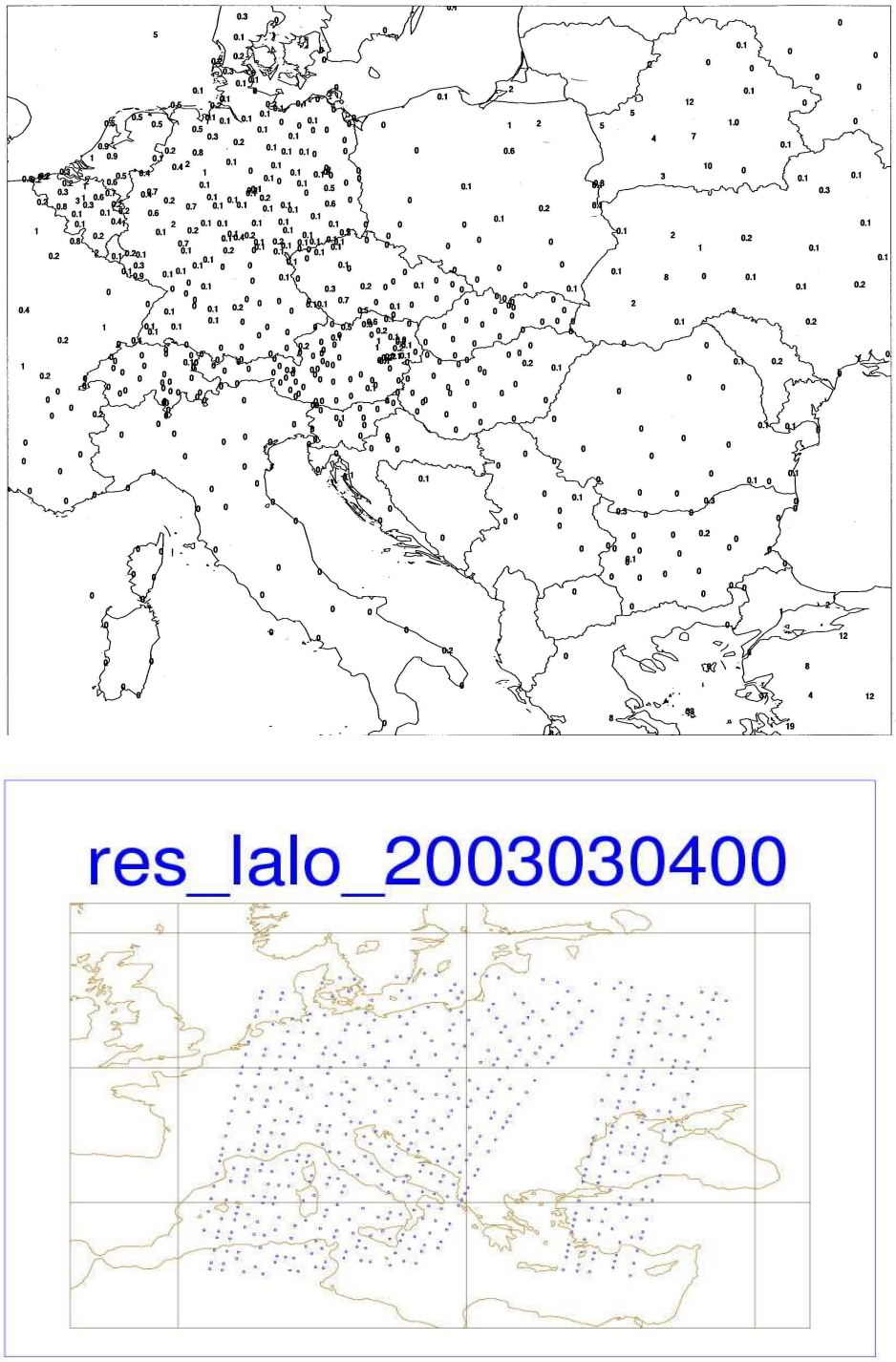

Figure 21: The 24 hour cumulative precipitation (in mm) extracted from SYNOP telegrams for 2003.03.05 06 UTC (upper picture) and the distribution of the ATOVS pixels at 2003.03.04 00 UTC (situation after screening - active observation) (lower picture).

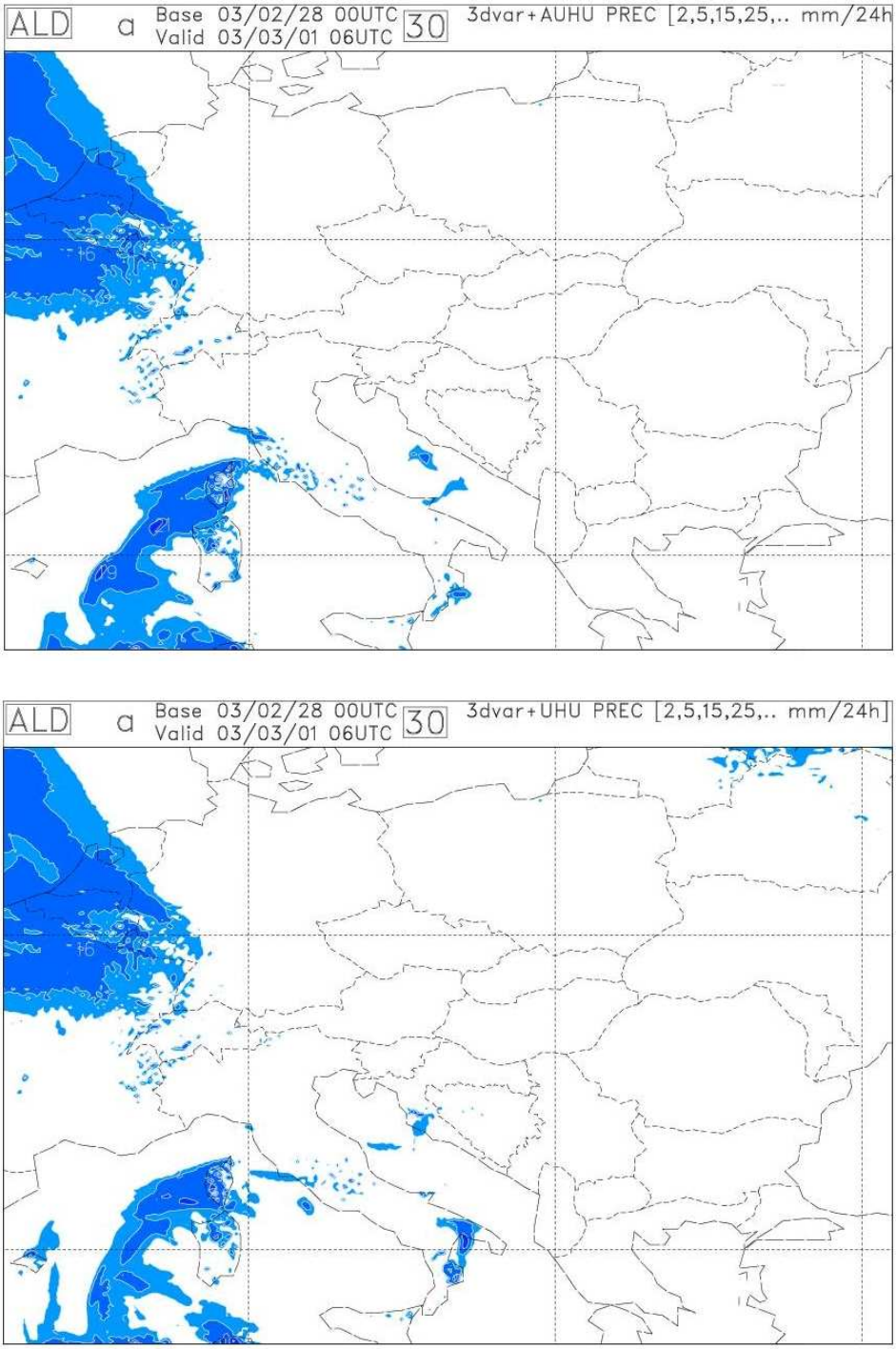

Figure 22: 24 hour cumulative precipitation (in mm) predicted over the ALADIN/HU domain from 2003.02.28 00 UTC. Upper picture: control run (with TEMP and SYNOP). Lower picture: 3D-Var run with ATOVS assimilated in 80 km resolution. In both runs the humidity was assimilated in univariate form. Note that the 24 hour cumulated precipitation is the difference between the cumulated precipitation predicted at 6 and 30 hour forecast ranges.

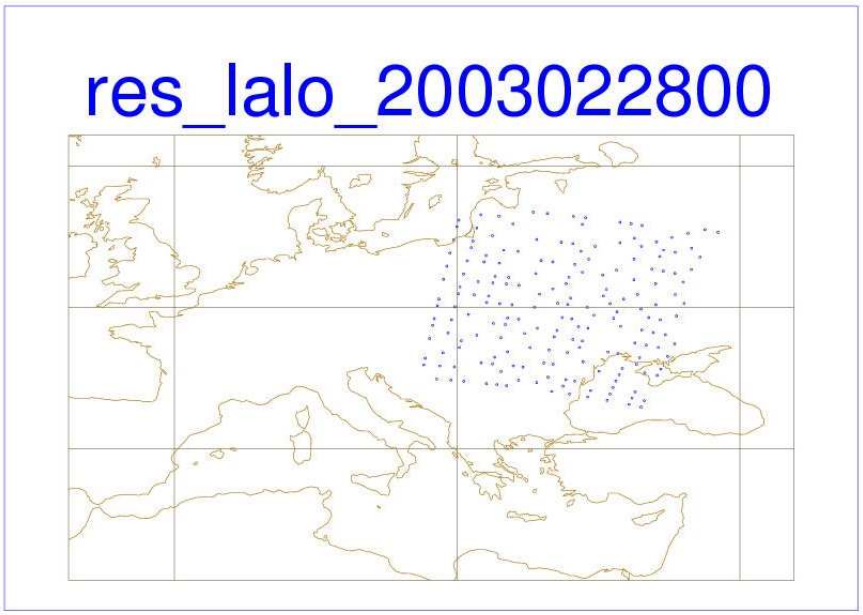

Figure 23: The distribution of the ATOVS pixels at 2003.02.28 00 UTC (situation after screening - active observation).

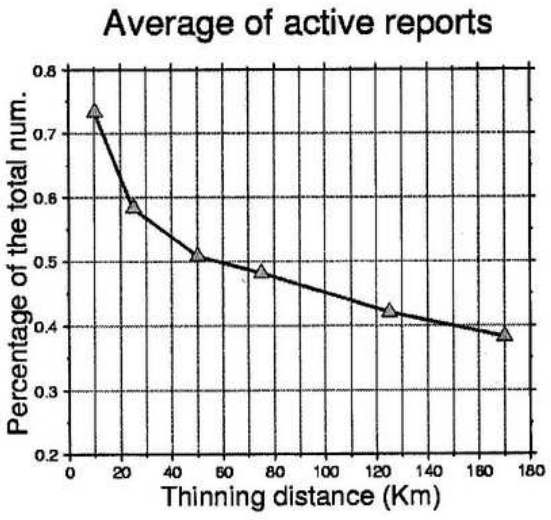

Figure 24: Percentage of active AIREP data at different thinning distances over the ALADIN France domaine

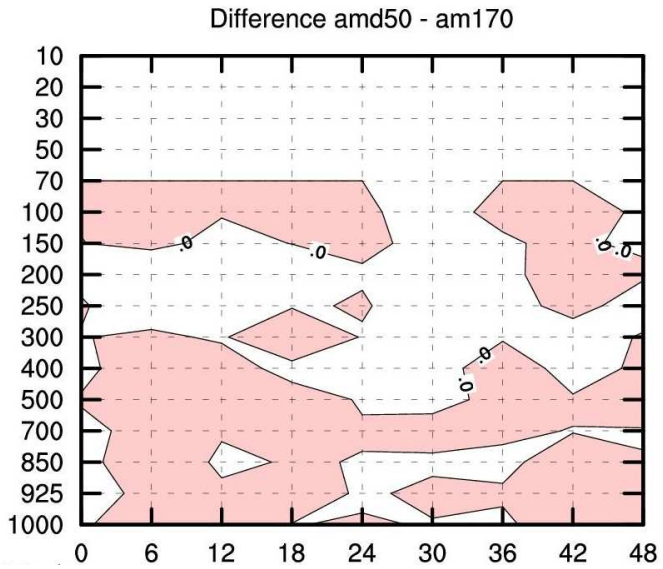

Figure 25: Difference between the root mean square errors for wind speed: $RMSE_{amd50} - RMSE_{am170}$. Negative value (coloured) means that the error of run with AMDAR data assimilated in 50 km resolution is less than that of AMDAR data assimilated in 170 km. X and Y axes present the forecast ranges and the model levels respectively.

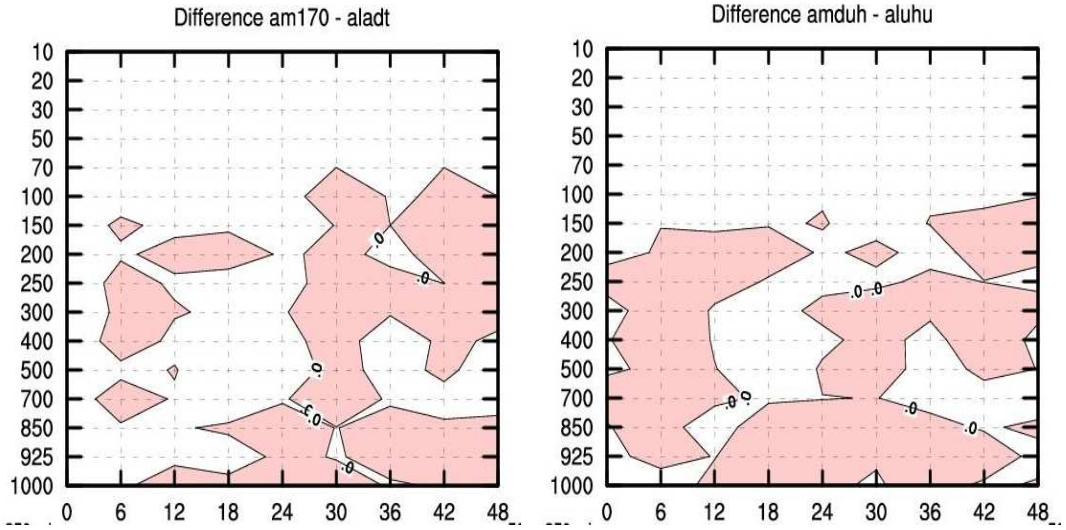

Figure 26: Comparison of the impact of the AMDAR data assimilated in 170 km resolution on wind speed, when assmilating the specific humidity with all control variables (left) and in univariate form (right). These graphs show the difference beetween the root mean square errors (with minus without). Coloured areas represent negative values.